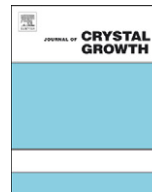




ELSEVIER

Contents lists available at [SciVerse ScienceDirect](http://www.sciencedirect.com)

Journal of Crystal Growth

journal homepage: www.elsevier.com/locate/jcrysgro

Effect of 8 MeV Si ions irradiation and thermal annealing in ZnO thin films

D.R. Hernández-Socorro^{a,*}, Z. Montiel-González^c, S.E. Rodil-Posada^c, L. Flores-Morales^b,
H. Cruz-Manjarrez^a, J.M. Hernández-Alcántara^a, L. Rodríguez-Fernández^a^a Instituto de Física, Universidad Nacional Autónoma de México, Ciudad Universitaria, México, D.F. 04510, México^b Facultad de Ciencias, Universidad Nacional Autónoma de México, Departamento de Física, Ciudad Universitaria, México, D.F. 04510, México^c Instituto de Investigaciones en Materiales, Universidad Nacional Autónoma de México, Ciudad Universitaria, México, D.F. 04510, México

ARTICLE INFO

Article history:

Received 20 August 2011

Received in revised form

11 May 2012

Accepted 13 May 2012

Communicated by M.S. Goorsky

Available online 4 June 2012

Keywords:

A1. Defects

A1. Ion beam

A1. Photoluminescence

A1. Spectroscopic ellipsometry

B1. Zinc oxide

B2. Semiconducting materials

ABSTRACT

ZnO thin films deposited by RF magnetron sputtering on silicon (100) wafers were irradiated by 8 MeV Si ions and thermal annealed in order to study optical properties. The presence of defects inside thin films as well as their implications was discussed by Photoluminescence and Spectroscopic Ellipsometry. Photoluminescence confirmed presence of energy states in forbidden band-gap associates with ultraviolet emission and Zn_i, O_i and O_{Zn} defects according to the treatment received. Spectroscopic Ellipsometry using the Tauc–Lorentz model plus a Lorentz oscillator was found to be the best model to describe the properties of irradiated samples that did not receive a second thermal annealing treatment. Through this model, it was possible to obtain optical band-gap in the range of 3.1–3.3 eV and excellent approximation of position in energy of the oscillator.

© 2012 Elsevier B.V. All rights reserved.

1. Introduction

Zinc oxide (ZnO) is a semiconductor with a band-gap greater than 3.0 eV and a large exciton binding energy of 60 meV at room temperature. There are several applications for ZnO thin films, such as transparent electrodes in optoelectronic devices [1,2], surface acoustic wave devices [2], varistors [1,3], heat mirrors for energy saving [4], solar cells [2,4], gas sensor [2,3], and blue and ultraviolet optical devices [5]. However, there is a lack of information concerning process–properties relationships. These relationships are quite important in developing ZnO-based devices. One remarkable aspect is the influence of defects caused by processes such as thermal annealing and ion irradiation on the electric and optical properties. There is a controversy about the nature of defects generated in as-deposited material and the ones induced after irradiation and/or thermal annealing.

Good quality ZnO films were grown through different methods, such as reactive thermal and electron-beam evaporation [6], sol–gel [7,8], pulse laser deposition [9], chemical vapor deposition [10], and magnetron sputtering [11]. Among all, magnetron sputtering showed several advantages, for example, low substrate temperature (down to room temperature), good adhesion

between film and substrate, scalability to large areas (upto $3 \times 6 \text{ m}^2$), great thickness uniformity with a deposition rate range (25–10,000 Å/min) and high film density [12–14]. For optical application a few microns of thickness are required to hold light wavelength for optical waveguides.

Ion irradiation of thin films is a process outside thermodynamic equilibrium which produces damage and structural changes unattainable through conventional techniques. Through high-energy-ion-trace some damage is produced mainly by electronic stopping. This damage causes modifications in films properties which depend on irradiation conditions (ion type, energy and fluence). Under controlled conditions this technique become promising for new materials synthesis, even more, considering that implantation and ion irradiation is widely applied in semiconductor industry [15]. Previously Muntele et al. reported morphological changes in ZnO films by 5 MeV Si ion irradiation [11].

The effect on optical properties of sputtered ZnO films through irradiation of 8 MeV Si ions and thermal annealing was analyzed in this research. Si ions at this energy are implanted in substrate at several microns deep. Then, it is possible to avoid the effects caused by Si impurities in the thin films. Photoexcitation, production and annihilation of defects and its influence in refractive index and band-gap were the properties analyzed. In order to characterize the films several techniques were used, for example,

* Corresponding author. Tel.: +52 55 56225160; fax: +52 55 56225009.
E-mail address: dhssocorro@yahoo.com.ar (D.R. Hernández-Socorro).

Rutherford Backscattering Spectrometry (RBS), Photoluminescence (PL) and Spectroscopic Ellipsometry (SE). All of them are well known for their precision and non-destructiveness.

2. Experimental details

ZnO thin films were deposited on the Si (100) substrates using RF magnetron sputtering. Target was ZnO with 99.99% purity and 5.0×10^{-2} m diameter. Target–substrate distance was 1.5×10^{-1} m. Deposition power (RF) was 117 W and deposition rate was 90 Å/min. After deposition, samples were thermally annealed (TA) and irradiated at 8 MeV Si^{+3} ions in a combination of different steps: as-growth (S1), as-growth plus irradiation (S2), as-growth plus irradiation plus TA (S3), as-growth plus TA (S4), as-growth plus TA plus irradiation (S5), and as-growth plus TA plus irradiation plus TA (S6). TA treatment was carried out at 773.15 K in air for 1 h in a Thermolyne furnace model 1400. Irradiations were conducted at fluencies of 1.0×10^{16} Si^{+3} ions/cm² using the electrostatic accelerator tandem Pelletron of 3 MV at Instituto de Física, UNAM.

Thickness and composition of films were obtained through RBS using 2 MeV $^4\text{He}^{2+}$ ions. RBS spectra were analyzed using the Rutherford Universal Manipulation Program (RUMP) software [16,17]. Optical investigation was carried out by PL and SE. PL emission spectra was obtained using a fluorescence spectrometer Perkin Elmer Precisely LS 55 equipped with a high energy pulse Xenon source. Measurement condition was excitation at 4.43 eV and filter at 3.55 eV. Ellipsometric measurements were obtained using a UVISSEL Jobin Yvon photoelastic modulated ellipsometer at 70° incidence angle. Ellipsometric data (I_s and I_c) were obtained in energy range of 1.5–5.0 eV using steps of 0.05 eV. Refractive index, extinction coefficient, band-gap and films thickness were obtained through spectra modeling.

3. Results

3.1. Rutherford Backscattering Spectrometry (RBS)

Fig. 1 shows a typical RBS spectrum of ZnO thin films on the Si substrate. The solid line corresponds to RUMP simulation. After a set of samples was analyzed, thicknesses between 170 and 180 nm, and stoichiometry composition of 1:1 were obtained. No changes of thickness and composition of samples under

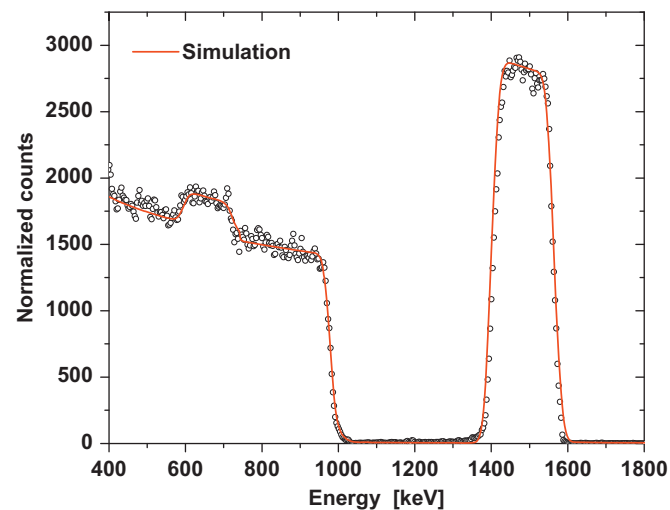


Fig. 1. Typical RBS spectrum for ZnO thin film on Si substrate. The solid line corresponds to RUMP simulation.

treatments were observed. This is an indication that under applied irradiation conditions (ion energy and fluence) sputtering effect is not detectable.

3.2. Photoluminescence (PL)

Emission properties of ZnO films are strongly related to growth conditions and post-treatment received. Room temperature PL spectra of the ZnO samples (S1–S6) are shown in Fig. 2. As-grown sample showed a wide peak where no clear emission line was identified. This behavior showed an electronic disorder as expected in a semiconductor grown at low temperature. After treatments the disorder was reduced and at least four principal emission peaks were observed [centered at 2.36 eV (green), 2.59 eV (blue), 2.97 eV (violet) and 3.18 eV (UV)]. Peak intensities depend on treatments received and ergo, on the defects production or annihilation.

3.3. Ellipsometry.

The Transparent Sellmeier and Tauc–Lorentz models were used in order to determine optical properties and films thickness of sample in study. The Transparent Sellmeier model was applied

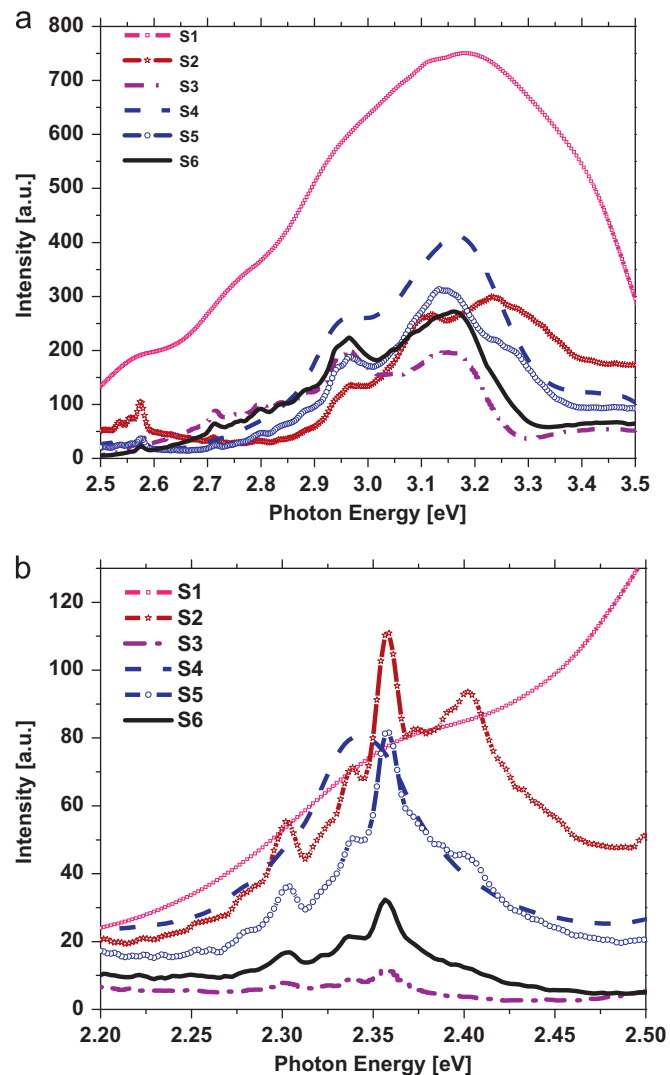


Fig. 2. Room temperature photoluminescence spectra: excitation at 4.43 eV and filter at 3.55 eV: (a) Area between 2.5 and 3.5 eV and (b) area between 2.2 and 2.5 eV.

in the transparent region (between 1.5 and 2.9 eV) to determine films thickness. Transparent region range was selected based on the fact that band-gap for ZnO is greater than 3.0 eV [4]. In addition, the Tauc–Lorentz model was used in the range of 1.5–5.0 eV to determine the optical properties where absorption processes take place.

An ellipsometric system records angles psi (Ψ) and delta (Δ) as a function of photon energy. These angles measures the changes in polarization state of the incident light upon reflection and are related to the Fresnel reflection coefficients by

$$\rho = \frac{r_p}{r_s} = \tan \Psi e^{i\Delta},$$

where r_p and r_s are the Fresnel reflection coefficients for p-polarized and s-polarized lights, respectively.

Original data obtained using photoelastic modulators are I_s and I_c , which are related to Ψ and Δ depending on the configuration used. Thus, in this case they are correlated as follows:

$$I_s = \sin(2\Psi)\sin(\Delta), I_c = \sin(2\Psi)\cos(\Delta).$$

For data analysis a four-layered model was applied as follows: (1) a Si substrate and (2) a 4.0 nm thick native oxide (SiO₂). Both layers were modeled using reference data from Palik [18]. Layer (2) was considered in the previous investigation where a clear improvement of fitting was obtained [19]. (3) A ZnO homogeneous layer (L_2) was modeled as described below and (4) a top layer (L_3) where a Bruggeman effective medium was used to model a porous ZnO film.

3.3.1. Optical analysis with the Sellmeier model.

ZnO optical properties were parameterized using a transparent Sellmeier model in sub band-gap region (1.5–2.9 eV) to estimate the film thickness. Sellmeier dispersion is an empirical model commonly used because of its good approximation to describe the spectral dependence of refractive index (n) in this region.

In this model the refractive index (n) is given by

$$n^2(\lambda) = A + \frac{\lambda^2 B}{\lambda^2 - \lambda_0^2}, \tag{1}$$

$$k(\lambda) = 0 \tag{2}$$

where λ is in nm. There are three fitting parameters: A , B , λ_0 .

Table 1 shows thickness and χ^2 (mean-square error standing where the best value is near to zero) of the Levenberg–Marquadt algorithm fit. A good fitting was obtained with exception of S2 and S5. For these samples χ^2 value was above three and the top layer has more than 50% of oxygen than zinc.

3.3.2. Tauc–Lorentz (T–L) model

The Tauc–Lorentz (T–L) model modified with the Lorentz oscillator was used in the 1.5–5 eV range to find optical properties

Table 1

Results of the Sellmeier model for all samples. The parameters shown are χ^2 (goodness of fit), L_2 (thickness of the ZnO dense layer), L_3 (thickness of porous ZnO layer), L_T (total thickness of $L_3 + L_2$ layers), and f_{ZnO} (volume fraction of ZnO in L_3 layer).

Samples	χ^2	L_2 (nm)	L_3 (nm)	L_T (nm)	f_{ZnO} (%)
S1	0.33	147.10	26.30	173.40	75.69
S2	14.40	142.00	44.70	186.70	2.93
S3	0.72	186.50	16.50	203.00	68.15
S4	0.58	144.80	25.20	170.00	86.82
S5	3.16	160.80	12.30	173.10	35.52
S6	0.93	174.40	15.30	189.70	63.97

of ZnO films. The T–L model was developed by Jellison and Modine [20]. Although the T–L model was initially proposed for amorphous semiconductors, different authors have shown that it is also suitable to describe the optical properties of ZnO films [21–25]. The T–L dispersion equations are given by

$$\varepsilon_2(E) = \begin{cases} \frac{AE_0C(E-E_g)^2}{(E^2-E_0^2)^2 + C^2E^2} \left(\frac{1}{E}\right) & (E > E_g) \\ 0 & (E \leq E_g) \end{cases} \tag{3}$$

$$\varepsilon_1(E) = \varepsilon_\infty + \frac{2P}{\pi} \int_{E_g}^{\infty} \frac{\xi \varepsilon_2(\xi)}{\xi^2 - E^2} d\xi \tag{4}$$

$$\varepsilon = \frac{f_j \omega_{oj}^2}{\omega_{oj}^2 - \omega^2 + i\gamma_j \omega} \tag{5}$$

The T–L dispersion model was obtained from the Tauc joint density of states and standard quantum mechanical or Lorentz calculation for ε_i (the imaginary part of the complex dielectric function) of a collection of non-interacting atoms. Eqs. (3) and (4) as a function of photon energy (E) are defined by five parameters: A (transition matrix element, which is proportional to the magnitude of ε_i , related to film density), E_0 (peak transition energy, corresponds to the Penn gap which represents an average separation between valence and conduction bands), C (broadening term, which can be related to the degree of disorder in the material), E_g (optical band-gap), all of which have the energy unit, and ε_∞ (high frequency dielectric constant), where P stands for the Cauchy principal part of the integral.

Lorentz oscillators' modification has been proposed to include discrete excitonic process [21]. Lorentz oscillator equations are given by

$$\varepsilon(E) = \varepsilon_0 + \sum_j \frac{A_j e^{i\varphi_j}}{E - E_j + i\Gamma_j} \tag{6}$$

$$\Gamma_j = \Gamma_0 - \frac{\Gamma_0 - \Gamma_0^{ex}}{j^2} \tag{7}$$

where four parameters are required for each oscillator included in the sum. Γ is the broadening parameter and the empirical expression is Eq. 7. A is a magnitude, which is proportional to the matrix element of the transition, and φ is the phase factor. Same four-layer system was used, but ZnO dense layer was modeled as described above. Each sample was modeled using a single T–L and T–L plus Lorentz oscillator. Results are shown in Table 2 and Fig. 3. The Fig. 3 shows how the fitting improved by

Table 2

Results of the T–L model and the T–L model plus Lorentz oscillator for all samples. The parameters shown are χ^2 (goodness of fit), E_g (optical band-gap), E_0 (location of T–L oscillator), E_1 (location of Lorentz oscillator).

Samples	χ^2	Tauc–Lorentz		Osc.
		E_g (eV)	E_0 (eV)	E_1 (eV)
S1	2.82	3.04	3.50	–
	1.72	3.06	3.58	3.49
S2	36.52	2.65	3.95	–
	7.50	3.21	3.17	3.25
S3	13.52	3.16	3.09	–
	4.91	3.09	2.57	3.42
S4	5.31	3.12	3.18	–
	1.65	3.17	3.21	3.42
S5	10.78	2.95	3.43	–
	1.81	3.26	3.28	3.45
S6	7.66	3.15	3.02	–
	2.11	3.11	3.31	3.84

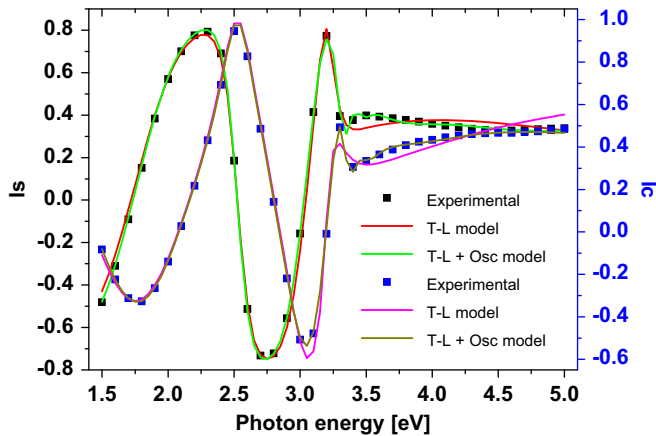


Fig. 3. Measured and calculated ellipsometric spectra for the T-L model and the T-L model plus Lorentz oscillator of S3 sample.

adding the Lorentz oscillator (S3 sample). This was the general trend for all samples as observed for χ^2 value in Table 2.

4. Discussion

RBS revealed that thickness and composition were not affected by annealing or irradiation or a combination of both treatments. PL spectra showed actual differences between as-grown (S1), thermal annealing (S4), irradiation (S2, S5) and irradiation plus second thermal annealing (S3, S6) samples, Fig. 2. Post-treatment samples show an ordering of electronic states less evident for the sample with only TA treatment. Two different deeds are presents in the ultraviolet region (> 3.1 eV): one peak around 3.1 eV for the samples with irradiation treatment at any step of the process and an additional peak at 3.24 eV for samples S2 and S5. Same case takes place in the green region (2.2–2.5 eV) where peaks are present at 2.30 eV, 2.33 eV, 2.36 eV and an additional peak at 2.4 eV for samples S2 and S5. Continuing the analysis, in the blue region (2.5–2.76 eV) there are some peaks because equipment light source has emissions at this energy. Meanwhile the violet region (2.76–3.1 eV) showed a strong peak centered at 2.96 eV. Emission peaks in the visible region are associated with states within band-gap. For example, a peak centered at 2.96 eV is caused by radiative defects Zn_i between this level and the conduction band; meanwhile, peaks in green region are associated with O_{zn} or O_i defects between this level and the valence band [5].

SE analysis for the transparent Sellmeier model showed that thickness of samples varied in the range of 170–203 nm, Table 1, this result matches with RBS data. The χ^2 value and volume fraction of ZnO in L_3 layer were acceptable for majority of samples. But this method fails for samples S2 and S5, associate with discrete excitonic process as a result of damage for irradiation treatment. These were described above as two additional peaks of PL. The T-L model itself does not sufficiently improve the fit process until the Lorentz oscillator was introduced in the model (Table 2). The χ^2 value improved in 50% for S2 and S5 samples, the optical band-gap value was in the range 3.1–3.3 eV and the position in energy of oscillator were excellent approximations that supported the model.

Fig. 4 showed that optical constant (n, k) has strong peaks around 3.3–3.5 eV. These peaks can be confirmed by excitonic transitions as reported by Yoshikawa and Adachi [21]. The n values were between 1.6 and 2.6 for the entire spectrum which is consistent with ZnO in bulk. Values of k higher than 0 in the range

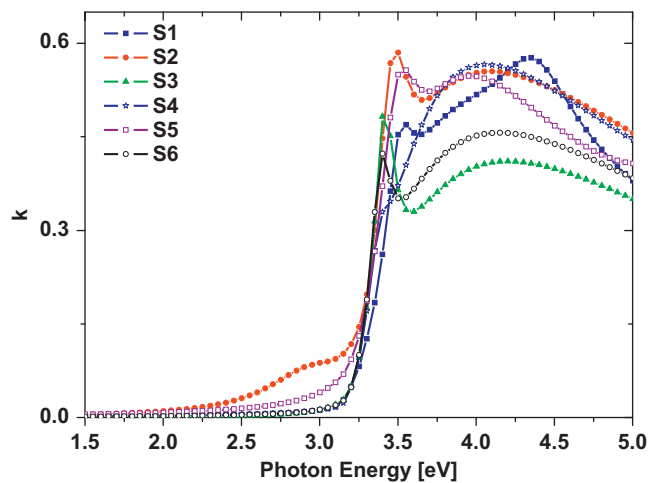
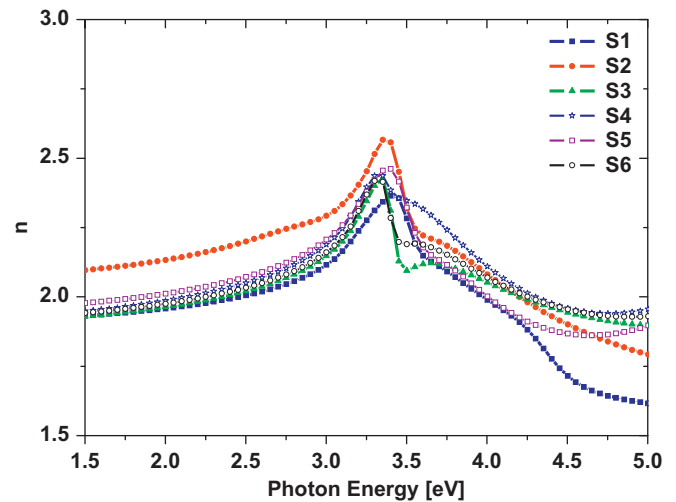


Fig. 4. Spectral of the complex refractive index, $N_i(E) = n_i(E) + jk_i(E)$ where $i=0,1$ and n , for ZnO thin films with all treatments in the entire energy spectrum (1.5–5 eV) for the T-L plus Lorentz oscillator model.

2.5–3.0 eV confirm that the transparent Sellmeier model cannot be used for S2 and S5 samples.

5. Conclusions

In conclusion, the characterization of ZnO thin films under irradiation with 8 MeV of Si and TA treatments is very important. Change in thickness or stoichiometry composition was reported for RBS technique. This fact means that ion energy and fluence applied does not have to consider the sputtering effect. A post-treatment process eliminates electronic disorder in semiconductors grown under low temperature condition. Extreme dependence between photoluminescence (PL) and samples' treatment was observed. The most significant defects inside the band-gap were Zn_i , O_i and O_{zn} and a new peak of PL was reported when samples received irradiation without second TA treatments. These peaks are associated with disorder in the region around ion trace that are removed by TA treatment support for bonding between Zn^{2+} and O^{2-} . The T-L model plus Lorentz oscillator is the best approximation for samples under irradiation and TA treatments. This new model is able to simulate discrete excitonic process as a result of damage for irradiation treatment. The use of this model is justified by the results found: χ^2 value improved in 50%, optical band-gap in range of 3.1–3.3 eV, a correct position in energy of

oscillator, n values in the range of 1.6–2.6 and extinction coefficient (k) values higher than zero for S2 and S5 which demonstrate non-transparency in the range 2.5–3.0 eV.

Acknowledgments

The authors thank F.J. Jaimes and K. López for their collaboration and operation of the Pelletron accelerator at Physic Institute, UNAM. We also want to thank J.G. Morales for the assistance in samples treatments. This work was supported by DGAPA-UNAM under Contract PAPIIT-IN109910 and ICYT-DF under Contract PICCO 10-75.

References

- [1] C. Jagadish, S. Pearton, Zinc Oxide Bulk, Thin Films and Nanostructures, Processing, Properties and Applications, Elsevier, 2006.
- [2] F. Chaabouni, M. Abaab, B. Rezig, Materials Science and Engineering B 109 (2004) 236–240.
- [3] R. Martins, E. Fortunato, P. Nunes, I. Ferreira, A. Marques, M. Bender, N. Katsarakis, V. Cimilla, G. Kiriakidis, Journal of Applied Physics 96 (2004) 1398.
- [4] E. Dumont, B. Dugnoille, S. Bienfait, Thin Solid Films 353 (1999) 93–99.
- [5] B. Lin, Z. Fu, Y. Jia, Applied Physics Letters 79 (2001) 943.
- [6] H.Z. Wu, K.M. He, D.J. Qui, D.M. Huang, Journal of Crystal Growth 217 (2000) 131.
- [7] T. Schuler, M.A. Aegerter, Thin Solid Films 351 (1999) 125–131.
- [8] M.N. Kamalasanan, S. Chandra, Thin Solid Films 288 (1996) 112–115.
- [9] W.S. Hu, Z.G. Liu, J. Sun, S.N. Zhu, Q.Q. Xu, D. Feng, Z.M. Ji, Journal of Physics and Chemistry of Solids 58 (1997) 853–857.
- [10] A.B.M.A. Ashrafi, N.T. Binh, B.P. Zhang, Y. Segawa, Journal of Applied Physics 95 (2004) 7738.
- [11] I. Muntele, P. Thevenard, C. Muntele, B. Chhay, R.L. Zimmerman, S. Sarkisov, D. Ila, Nuclear Instruments and Methods in Physics Research B 242 (2006) 512–516.
- [12] R. Hong, H. Qi, J. Huang, H. He, Z. Fan, J. Shao, Thin Solid Films 473 (2005) 58–62.
- [13] K. Ellmer, Journal of Physics D Applied Physics 33 (2000) R17.
- [14] R.F. Bunshah, Handbook of Deposition Technologies for Films and Coatings, Science, Technology and Applications, Noyes Publications, 2005, pp. 12 and 142.
- [15] E. Knystautas, Engineering Thin Films and Nanostructures With Ion Beams, Taylor & Francis, 2005 Ed.
- [16] Official website of RUMP software. <<http://www.genplot.com/>>.
- [17] L.R. Doolittle, Nuclear Instruments and Methods B 15 (1986) 227.
- [18] E.D. Palik, Handbook of Optical Constants of Solids, Elsevier, 1998.
- [19] Q.H. Li, D. Zhu, W. Liu, Y. Liu, X.C. Ma, Applied Surface Science 254 (2008) 2922–2926.
- [20] G.E. Jellison, F.A. Modine, Applied Physics Letters 69 (1996) 371.
- [21] H. Yoshikawa, S. Adachi, Japan Journal of Applied Physics 36 (1997) 6237.
- [22] H. Fujiwara, M. Kondo, Physical Review B 71 (2005) 075109.
- [23] S.H. Mohamed, S.A. Ahmed, European Physical Journal of Applied Physics 44 (2008) 137–141.
- [24] C. Koidisa, S. Logothetidis, A. Laskarakisa, I. Tsiaoussisa, N. Frangis, Micron 40 (2009) 130–134.
- [25] E. Çetinörgü, S. Goldsmith, R.L. Boxman, Thin Solid Films 515 (2006) 880–884.